Electromechanical Behavior and Environmental Resistance of Laser-fabricated Oxides on Stainless Steel

SAND2013-4983C

PURDUE ENGINEERING MATERIALS ENGINEERING

S.K. Lawrence[1,2*], D.P. Adams[2], D.F. Bahr[1], N.R. Moody[2]

1. Purdue University ; *First year SSGF Fellow; 2. Sandia National Laboratories

Sandia National Laboratories

Objective & Characterization Methods

Nanosecond pulsed laser irradiation of *stainless steel 304L* substrates leads to the growth of highly colored oxide films for use as passive indicators of tamper in welded or sealed components of energy systems. Microscopy and diffraction techniques were used to characterize the morphology, microstructure, and phase of the oxides. Mechanical behavior, fracture, and electromechanical characteristics of the films were investigated with a variety of nanoindentation techniques. Environmental resistance was evaluated with immersion testing followed by focused ion beam sectioning and energy dispersive spectroscopy.

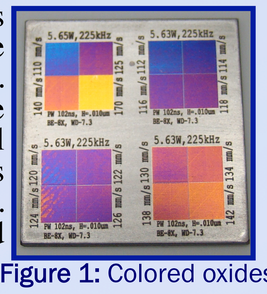

Figure 1: Colored oxides.

Oxide Phase & Morphology

5º grazing incidence x-ray diffraction and multiscale microscopy reveal formation of multiple oxides with composition gradients and highlights distinct morphology and microstructure.

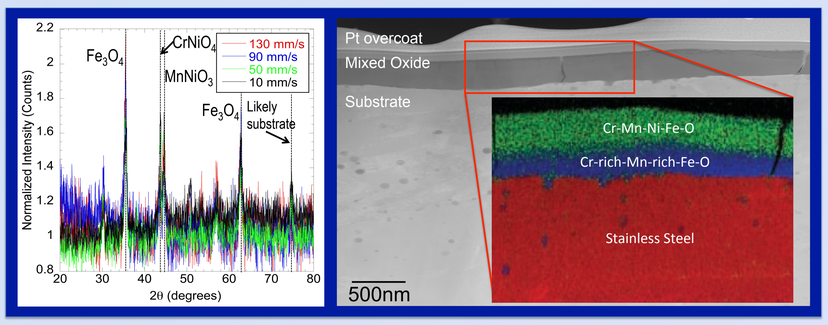

Figure 2: GIXRD of 250kHz SS oxides (left). Peak ID indicates predominant oxides are Fe_3O_4 and a Cr-Ni-Fe oxide. STEM EDS (right) reveals a sharp interface between substrate and oxide, but two distinct phases in the oxide with a composition gradient between the interfacial layer and overlayer.

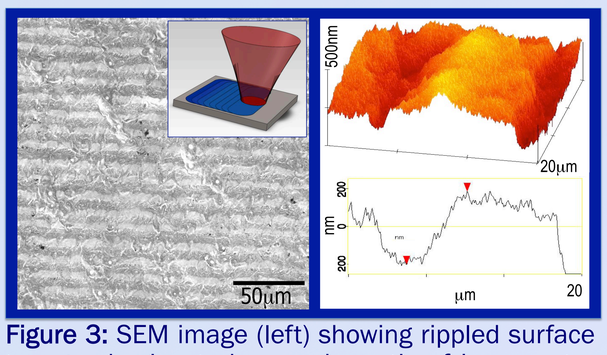

Figure 3: SEM image (left) showing rippled surface topography, inset shows schematic of laser raster resulting in ripples. AFM image (right) of a single ridge-valley period leading to large scale ripples.

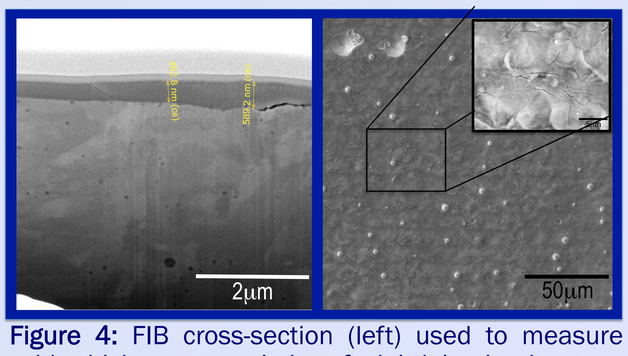

Figure 4: FIB cross-section (left) used to measure oxide thickness reveals interfacial delamination; top-down SEM (right) shows pervasive surface cracks formed to relieve residual film stress post-processing.

Oxide Mechanical Properties & Fracture Behavior

Dynamic nanoindentation yielded modulus, hardness, and stiffness values. High-load quasi-static (QS) conical indentation was used to determine load/depth at oxide fracture events.

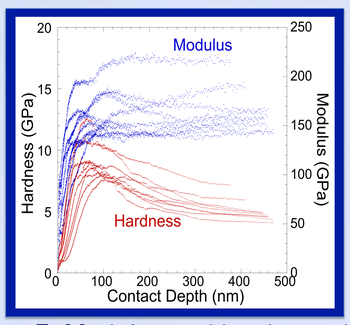

Figure 5: Modulus and hardness data.

Table 1: Average modulus and hardness data. Values are means of maximums, averaged over all four scan rates per frequency.

Laser Scan Rates (mm/s)	*Pulse Frequency (kHz)*	*Hardness (GPa)*	*Modulus (GPa)*
30, 47, 80, 175	225	9.2±2.1	155±25
10, 50, 90, 130	250	8.8±2.1	145±39
10, 50, 90, 130	275	11.6±3.5	166±32
40, 50, 60, 70	350	11.4±2.6	198±43

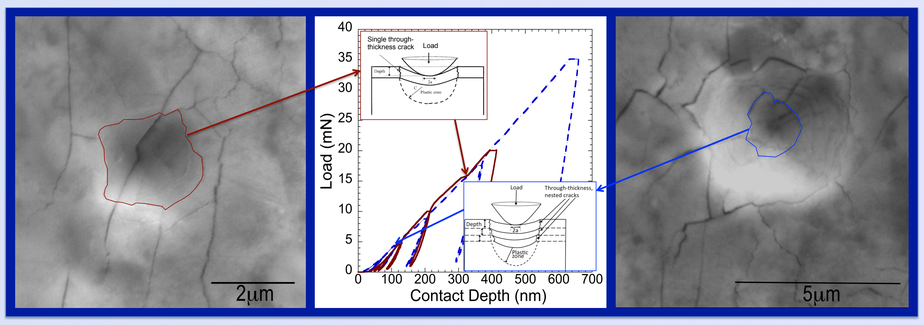

Figure 6: Circumferential cracks at contact radius correspond to load-depth excursions at higher loads (left), while inner, nested cracks in high-load indents correlate with excursions at low loads (right). Schematics are shown in insets (middle).

Figure 7: Cumulative distribution plot of fracture loads (determined from excursions in conical tip load-depth data like that shown in middle plot of Fig. 8). The critical load required to cause fracture is a function of processing parameters: faster laser scan rates require a higher applied load to cause through-thickness fracture. Similarly, faster laser scan rates have higher maximum fracture loads than their slower counterparts. Since load at fracture can be used to calculate fracture toughness, Fig. 7 indicates there should be a correlation between processing parameters and fracture toughness.

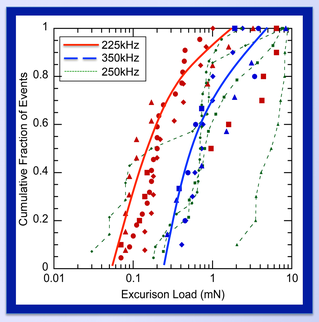

Oxide Electromechanical Properties

Conducting nanoindentation measured current response to voltage sweeps and indicates a correlation between laser exposure, current-voltage behavior at a constant load of 10mN.

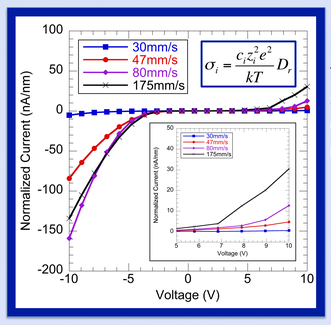

Figure 8: Polarization curves for 225kHz oxides, normalized by thickness. Conductance is not a function of thickness, thus the dependence on scan rate must be linked to defect density. Inset equation links conductance, σ_i, with defect concentration, c_i.

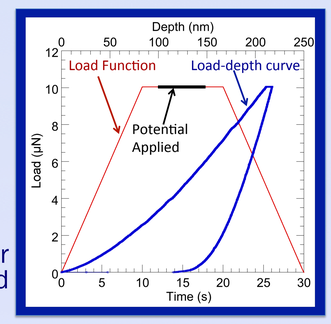

Figure 9: Loading regime used for conducting indentation, showing applied potential and resulting load-depth record.

Oxide System Environmental Resistance

Oxided areas were isolated then submerged in a 3% NaCl solution (simulated sea water) for 25 days. Uniform corrosion product indicates exposure of an altered substrate.

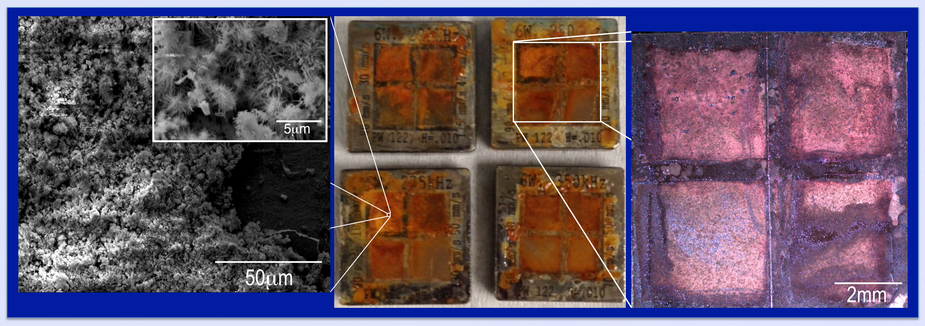

Figure 10: Post-immersion optical image (middle); of corrosion product covers oxides. SEM image of corrosion product on oxide area (left), inset shows structure of product; (right) higher magnification optical micrograph indicates corrosion product is not well-adhered.

Figure 11: Deposition of a uniform corrosion product suggests substrate composition is altered. FIB cross-sectioning (left) followed by EDS dot-mapping reveals a Cr-gradient between the bulk substrate and oxide layers. Overlayed Fe-Cr and O-Cr maps (middle) show development of layers, while individual element dot maps indicate relative amounts and areas of intensity for Fe, Cr, O used to create overlap maps.

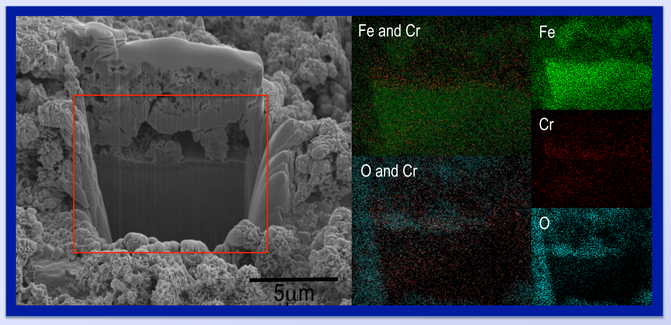

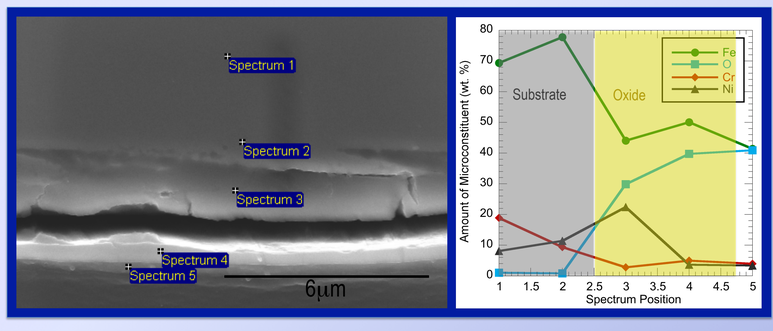

Figure 12: Metallographic cross sections examined with EDS spot profiles provide a semi-quantitative analysis of microconstituents. Cr content decreases near the substrate-oxide interface and then increases slightly in the oxide (positions shown on left, amounts in plot on right). Depletion of Cr increases susceptibility to seawater attack.

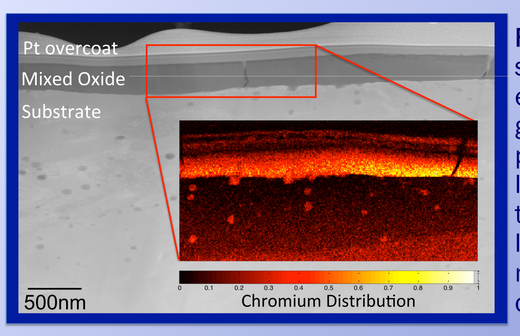

Figure 13: STEM EDS of an oxide-substrate interface which was not exposed to salt water also reveals a Cr gradient, further corroborating the proposal that substrate heating during laser processing results in Cr diffusion through the bulk substrate into the oxide leading to a Cr-depleted, "sensitized-like" microstructure immediately beneath the oxide that is prone to sea water attack.

Conclusions

- **Oxides grown via nanosecond pulsed laser irradiation are composed of multiple phases. High residual stresses from formation are relieved through oxide delamination and through-thickness cracking.**
- **Hardness and elastic modulus of oxides on SS 304L are ~12GPa and 160GPa, respectively, and are relatively insensitive to processing parameters. However, faster laser scan rates (i.e., lower laser fluence) lead to oxides that fracture at higher loads for a given contact probe.**
- **Conducting nanoindentation manifests a unique correlation between laser processing parameters and oxide conductivity—faster laser scan rates correspond with higher conductivity, likely due to the presence of point defects such as vacancies as well as large defects such as through-thickness cracks.**
- **Immersion in simulated seawater results in corrosion of the steel immediately beneath oxides, indicating surface cracks are through-thickness and substrate composition is altered during processing. Multiscale EDS reveals Cr-depletion, increasing susceptibility to seawater attack, at all processing parameters.**

Acknowledgements

Many thanks to Vitalie Stavila, Mark Rodriguez, and Ray Friddle for their work and helpful discussions on microscopy and XRD.

This work was supported by the Defense Threat Reduction Agency, Basic Research Award # IACRO 11-4471I, to Purdue University sub-contracted through Sandia National Laboratories and NSF Grant NSF/DMR-0946337.